Electronic Supplementary Information (ESI)

All-porous heterostructure of reduced graphene oxide-polypyrrole-nanoporous gold for planar flexible supercapacitor showing outstanding volumetric capacitance and energy density

Taniya Purkait, Guneet Singh, Navpreet Kamboj, Manisha Das, Ramendra Sundar Dey*

Institute of Nano Science and Technology (INST), Mohali-160064, Punjab, India.

Email: rsdey@inst.ac.in

Materials and chemicals

Highly pure graphite flakes (<20μm), phosphorous pentoxide (P_2O_5, >98%), potassium permanganate ($KMnO_4$), copper sulphate ($CuSO_4$), Tetraethylammonium tetrafluoroborate (Et_4NBF_4), ethylene carbonate (EC), and dichloroethane (DCE) were purchased from Sigma Aldrich and were used as received. Sulphuric acid (H_2SO_4), nitric acid (HNO_3), hydrochloric acid (HCl), and perchloric acid ($HClO_4$) were purchased from Merck chemicals India. Poly (vinyl) alcohol (M.W. 89000-98000) was purchased from Alfa Aesar (Thermo Fischer Scientific Chemicals Inc.; US). Pyrrole was obtained from TCI chemicals and was used as received. were purchased from Sigma-Aldrich. A 12ct silver/gold (Ag/Au) alloy foil having a content ratio of 1:1 was purchased from Goodfellow Manufacturer & Supplier, USA. PET sheets (d = 0.3 mm) were purchased from local market. Before use, all the PET sheets were washed with de-ionised (DI) water and then plasma treated to generate surface functionalities. All other chemicals used were at least of analytical grade and were used without any further purification. All aqueous solution was prepared using Millipore water.

Characterization of materials

Electrochemical measurements like cyclic voltammetry, galvanostatic chargedischarge, Electrochemical Impedance Spectroscopy (EIS), etc. were performed on a CHI 760E electrochemical workstation. During electrodeposition of three dimensional porous reduced graphene oxide (3DrGO) networks, nanoporous gold lectrode (npAu) was assigned as the working electrode while the as deposited 3DrGO/npAu was chosen as the working electrode for the simultaneous electropolymerization and constant potential deposition of polypyrrole (PPy). In all cases, counter electrode was a platinum wire while all calculations were made against the Ag/AgCl (3 M) electrode that was selected as the reference. However, all the electrochemical performances of the in-plane microsupercapacitor device were tested in two-electrode setup using solid state gel electrolyte. Mass loading of the active electrode material on the npAu substrate was calculated using an electrochemical quartz crystal microbalance (EQCM) analysis available on Metrohm Autolab PGSTAT instrument. X-ray Diffraction (XRD) spectroscopic study was carried out on a Bruker D8 Advances instrument using Cu-Kα (λ = 1.5406 Å) radiation in the 2θ range from 5° to 80° with an acceleration voltage of 40 KV. Raman Spectroscopy was performed on a WITEC Focus Innovations Alpha-300 Raman confocal microscope at a laser wavelength of 532 nm. Nitrogen adsorption-desorption analysis was done at 77 K on an Autosorb iQ2 instrumental setup to examine the surface area by Brunauer Emmett Teller (BET) method. The samples were degassed at 150 °C for more than 12 h under vacuum conditions. The surface morphology and the elemental composition of the synthesized material were investigated using Scanning Electron Microscopy (SEM Jeol JSMIT300) equipped with a Bruker XFlash 6130 Energy Dispersive X-ray Spectroscopy (EDS). X-Ray photoelectron (XPS) spectroscopy was performed on a KAlpha plus XPS system by ThermoFisher Scientific instruments in an ultrahigh vacuum chamber (7X10-9 torr) using Al Kα radiation (1486.6 eV). The interdigitated in-plane microfinger arrays were patterned on the as deposited active electrode materiala using Trotec Laser engraver system. A near infra-red (NIR) Laser source with a power of 10 W has been used for scribing. Surface profiling was carried out on a Bruker DektakXT Stylus Profiler to measure the

thickness of the deposited electrode material. The electrical conductivity of the hybrid material was measured by a two-probe method using a Keithley 2635B source meter.

Calculations and formulas of all-solid-state microsupercapacitor:

The specific capacitance (C_{SP}) can be calculated from cyclic voltammetry via the equation (1)

$$C_{SP} = \frac{1}{2\langle A|V|M\rangle \nu (V_f - V_i)} \int_{V_i}^{V_f} I(V)dV \qquad (1)$$

where A (in cm^2) is the geometric area, V is the overall volume and M (in g) is the active electrode mass of the active electrodes as calculated from EQCM measurements in both two and three electrode setups, ν is the voltage scan rate, V_f and V_i (in V) are the potential limits of the CV curves, and I(V) is current at different potentials. $\int_{V_i}^{V_f} I(V)dV$ is the numerically integrated area of the CV curves of the electrode materials interdigitated onto the electrode surface.

Alternatively, the specific capacitance, C_{SP} can also be calculated from galvanostatic charge-discharge curves by equation (2) as following

$$C_D = \frac{I\Delta t}{\Delta V} \frac{1}{\langle A|V|M\rangle} \qquad (2)$$

where, I (in A) is the discharge current, Δt (in s) is the discharge time, A (in cm^2) is the overall geometric area of the device (calculated from SEM), V (in cm^3) is the overall volume of the device (calculated from SEM as well as surface profilometer), M (in g) is the active electrode mass and, ΔV (in V) is the working voltage.

The equation can express the energy density (E) and power density (P) of a supercapacitor device, (3) moreover, (4) as following

$$E = \frac{\Delta V^2}{2\times 3600} (C_{sp})_{\langle A|V|M\rangle} \quad (3)$$

$$P = \frac{E \times 3600}{\Delta t} \qquad (4)$$

Where $(C_{sp})_A$, $(C_{sp})_V$ and $(C_{sp})_M$ is the areal, volumetric and gravimetric capacitance of the active electrodes as well as the all solid-state in-plane MSC device, respectively.

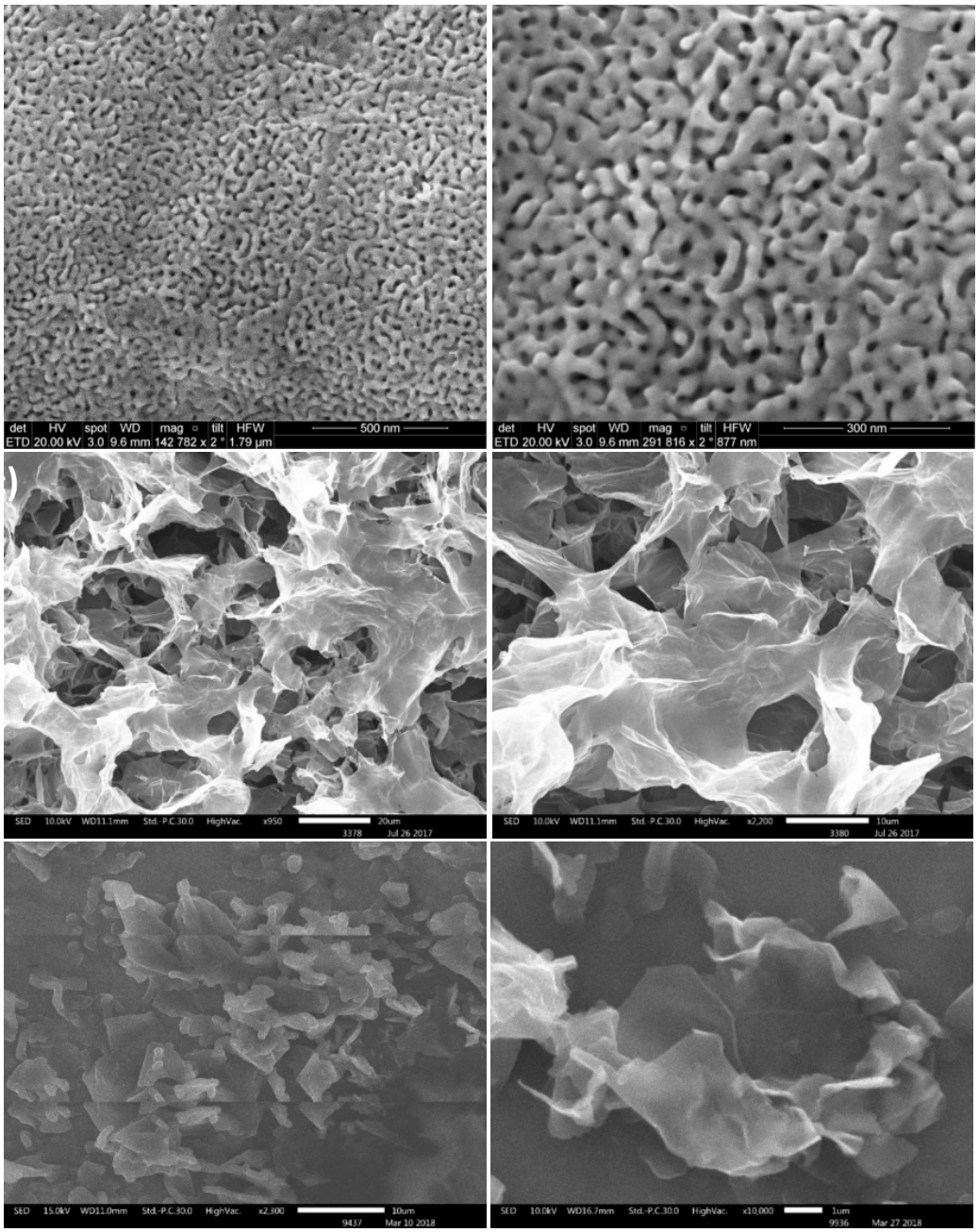

Figure S1. Microscopic images of the surfaces of the current collector and the active electrode materials on the current collector; **(a)-(b)** npAu, **(c)-(d)** 3DrGO/npAu and **(e)-(f)** PPy/npAu electrodes (top view) at various resolutions. Scale bar: 300 nm, 500 nm, 1 µm, 10 µm, 20 µm.

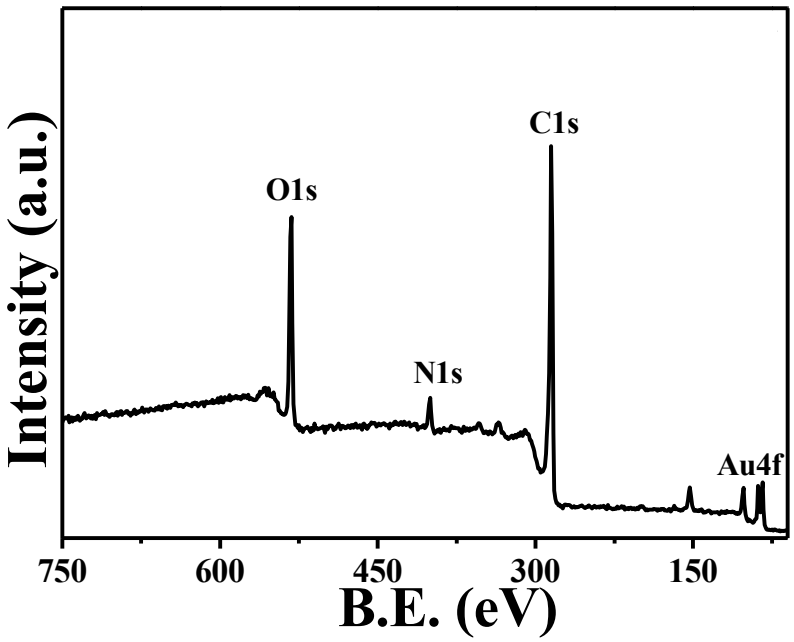

Figure S2. The overall XPS spectra of the PPy-3DrGO hybrid material on npAu substrate.

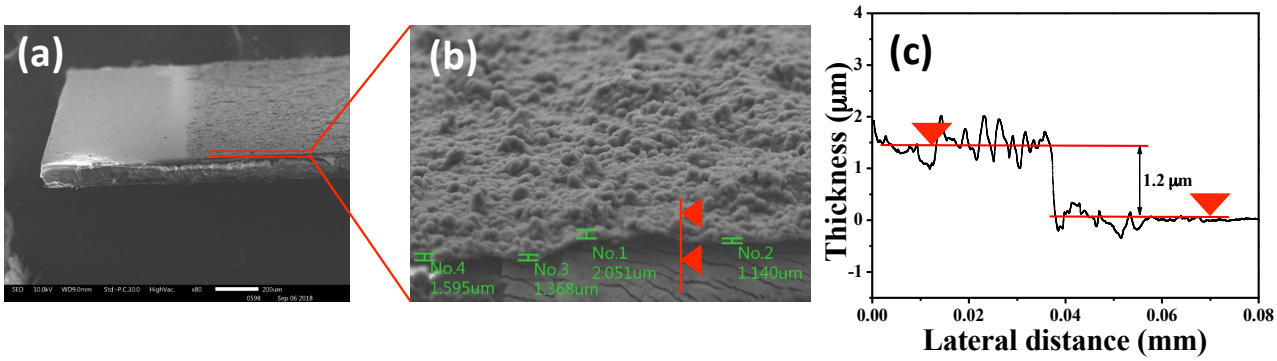

Figure S3. (a) Cross-sectional SEM images of the PPy3DrGO/npAu based electrode surface, deposited on a PET substrate; **(b)** magnified view showing average thickness of the deposited hybrid material on the current collector **(c)** Surface profiling of the selected area shows material thickness to be around 1.2 µm. (Red probes are shown in (b) and (c) for the representations only)

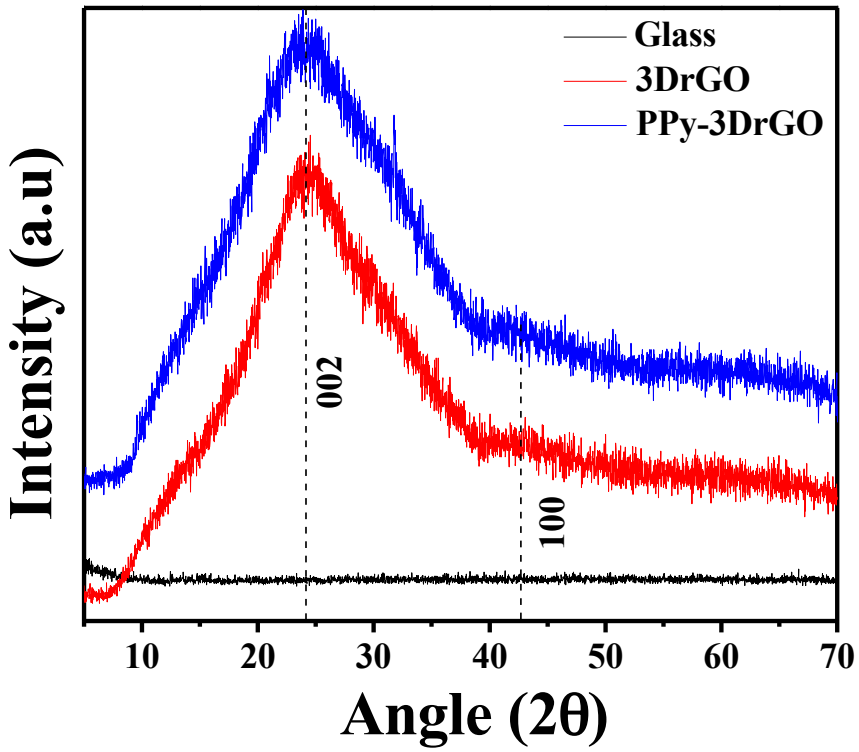

Figure S4. XRD spectra of the active materials, 3DrGO and PPy-3DrGO on a glass substrate.

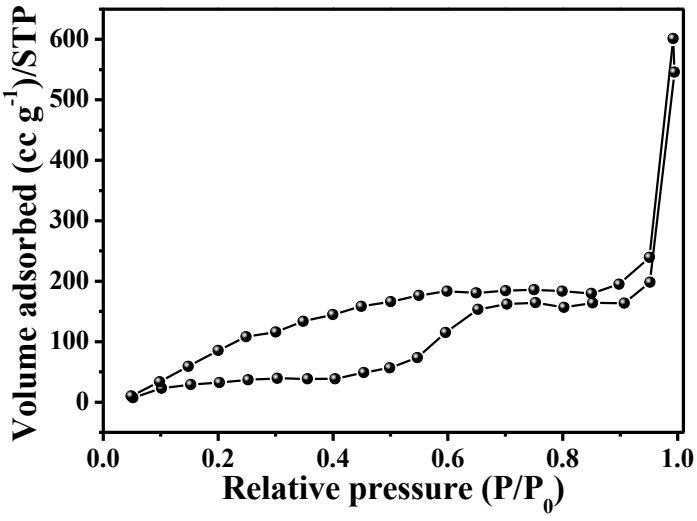

Figure S5. BET surface area analysis of the hybrid material, PPy-3DrGO by N_2 sorption analysis isotherm.

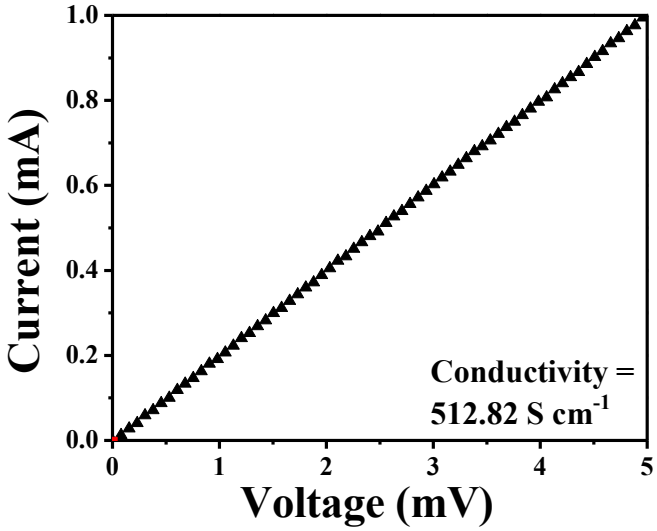

Figure S6. Electrical conductivity measurement (I-V characterization) of the hybrid material, PPy-3DrGO on npAu current collector via two-probe method.

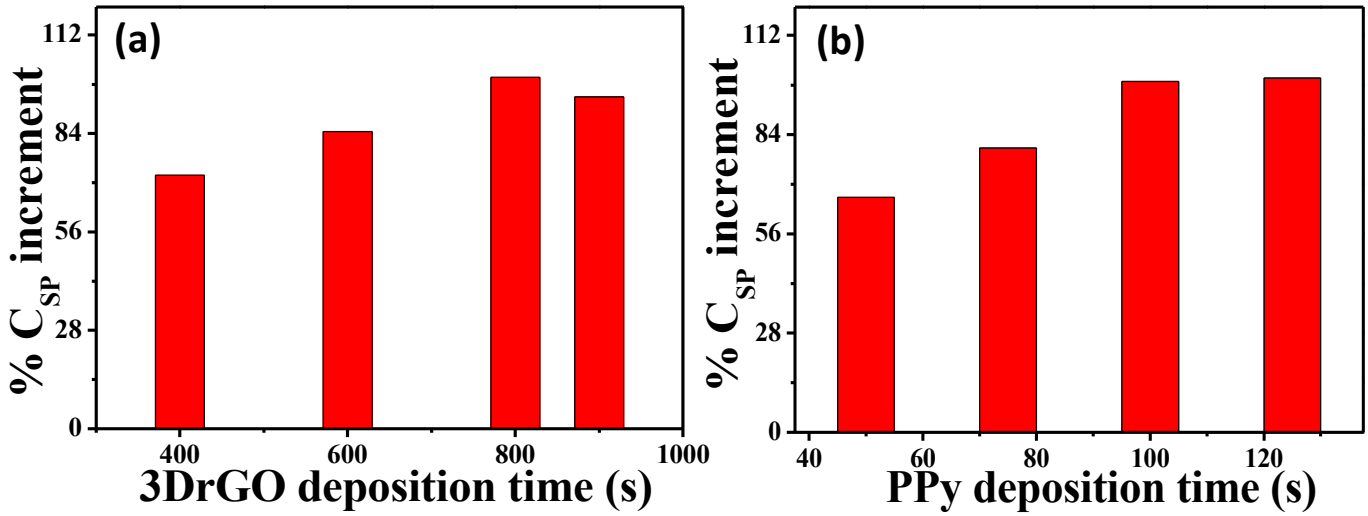

Figure S7. Effect of concentration of the analyte on the percentage specific capacitance of the developed PPy-3DrGO hybrid electrode material (a) 3DrGO; (b) PPy.

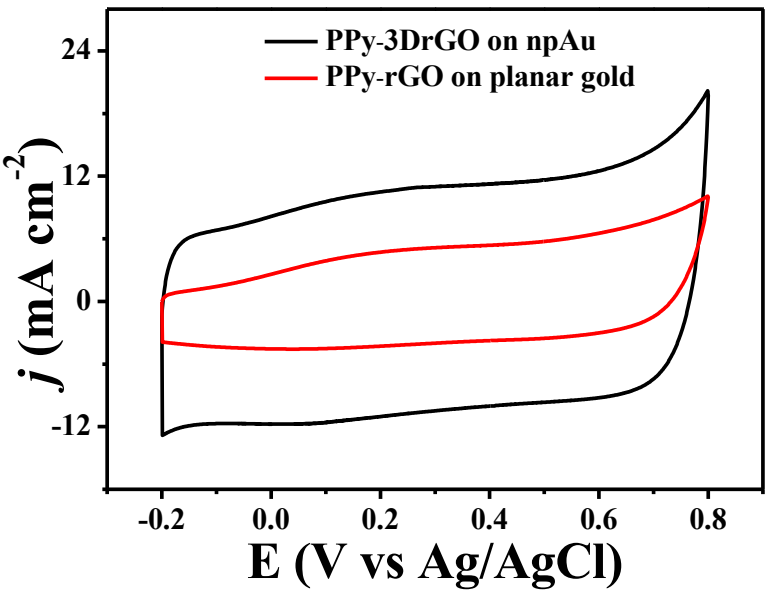

Figure S8. Comparative cyclic voltammetric analyses showing the influence of npAu as compared to a planar gold substrate in increasing the capacitive properties of the reduced graphene oxide-conducting polymer (PPy-3DrGO) composite material.

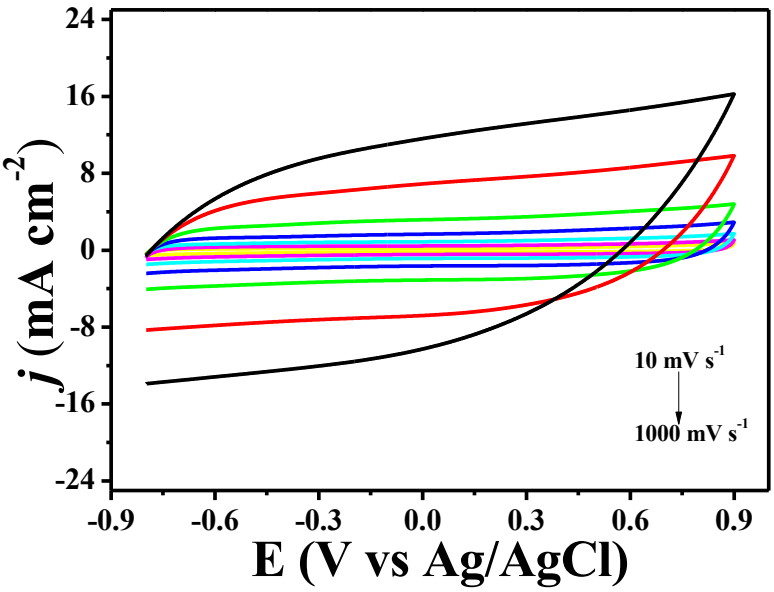

Figure S9. CV analysis showing retention of voltammogram shapes of the all-solid-state in-plane MSC based on Ppy-3DrGO composite material even at high scan rates.

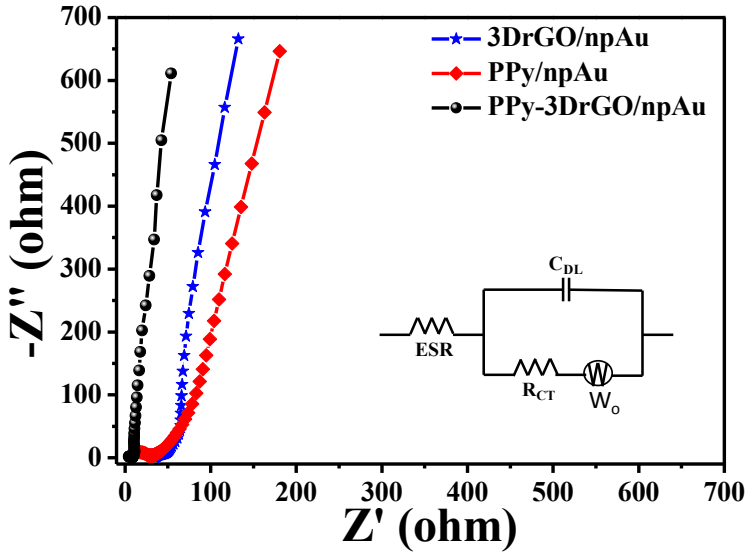

Figure S10. Comparative Nyquist plot showing enhanced capacitive property of the PPy-3DrGO composite material. Inset shows the equivalent circuit used to fit the EIS spectra).

Table S1. Summarized equivalent circuit parameters from fitted Nyquist plot.

Electrode	ESR (Ω)	R_{CT} (Ω)	C_{DL} (F)	W_0	
				n	A (Ω S^{-n})
3DrGO	32.94	9.9793	0.0005	0.65	75.12
PPy	16.56	36	0.000425	0.68	391.18
PPy-3DrGO	4.2	7.7932	0.00032	0.45	11.88

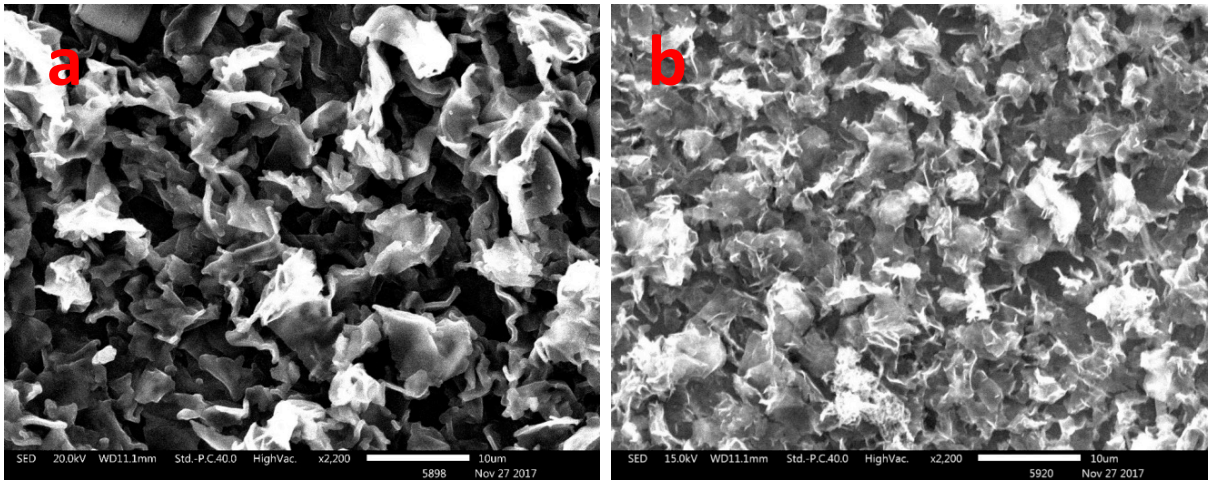

Figure S11. SEM images of the solid-state symmetric supercapacitor electrode surface obtained **(a)** before and **(b)** after 10000 cycles of charge-discharge at a high current density of 5 mA cm^{-2}.

Supporting video 1. Supporting video describes the mechanical flexibility of the in-plane symmetric microsupercapacitor device. Cyclic voltammetric response was recorded while continuously bending the device at various angles and compared with the device response in a straight mode.

Supporting video 2. Supporting video describes the performance and output deliverance of the in-plane symmetric microsupercapacitor device after charging it for 2 minutes at 3 V, the discharging performance of the device was monitored for at least 30 minutes.